Dalton Transactions

An international journal of inorganic chemistry

www.rsc.org/dalton

Number 44 | 28 November 2009 | Pages 9661–9936

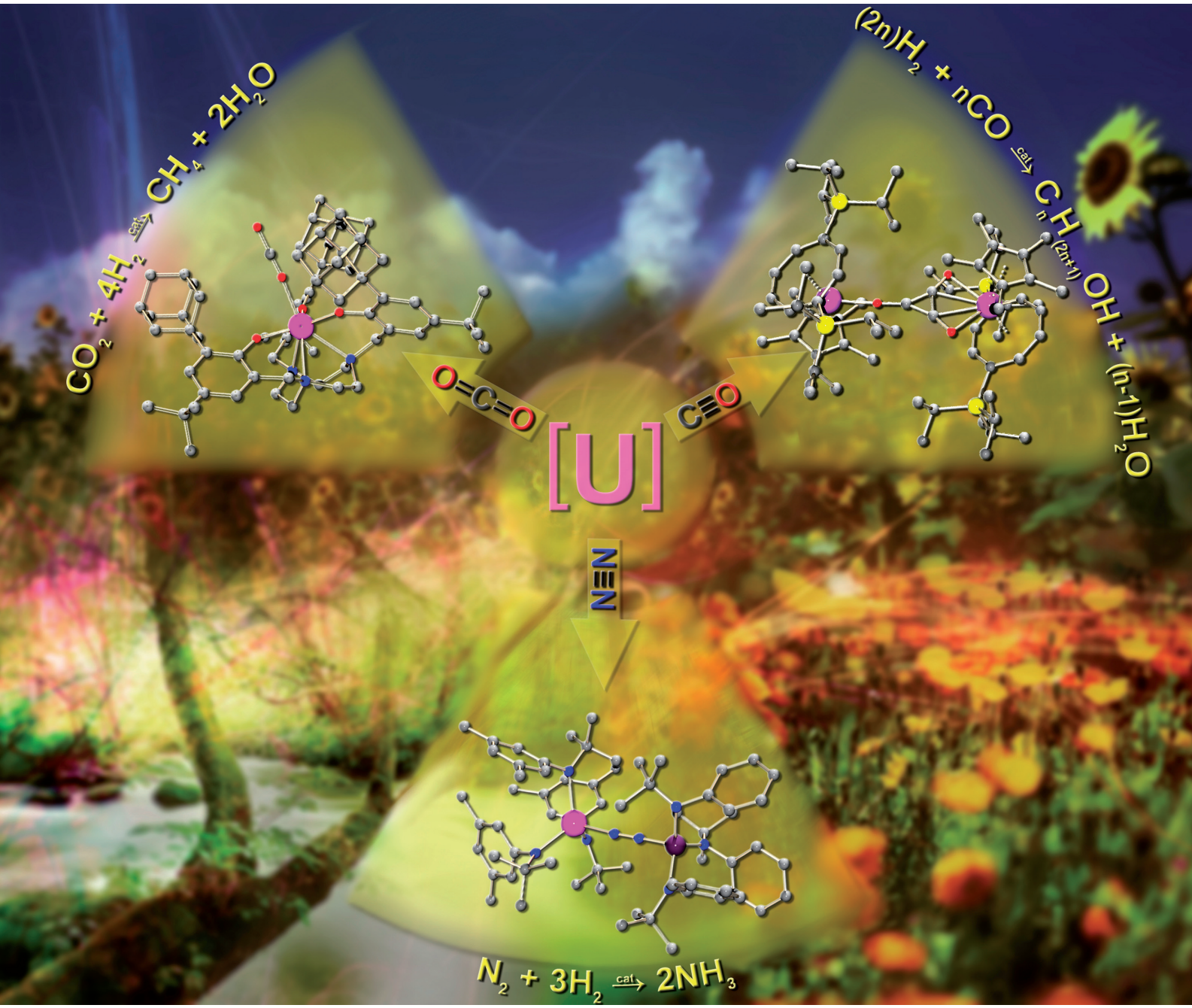

ISSN 1477-9226

RSC Publishing

1477-9226(2009)44;1-V

Influence of steric pressure on the activation of carbon dioxide and related small molecules by uranium coordination complexes

Oanh P. Lam,[a,b] Christian Anthon[a] and Karsten Meyer*[a]

Received 23rd March 2009, Accepted 14th May 2009
First published as an Advance Article on the web 23rd July 2009
DOI: 10.1039/b905537a

Recent reports on new types of reactions and bonding using uranium coordination complexes have marked uranium as an effective candidate for small molecule activation and potentially as a key participant in catalytic processes. This review discusses the advantages of employing uranium in coordination chemistry, with emphasis on the importance of ligand design and the promotion of unusual chemical transformations by steric pressure. The activation of industrially relevant C1 feedstocks such as CO and CO_2 by uranium complexes with their exemplary abilities to stabilize highly reactive charge-separated complexes are highlighted in this article. Spectroscopic and DFT studies are also presented, demonstrating the important methods that are utilized for investigating the electronic properties of these uranium complexes.

1. Introduction

Few elements experience the Jekyll and Hyde reputation that uranium does. On one hand, the research community has been compensated with numerous exciting discoveries of new types of reactions,[1–6] bonding,[2,7–9] and even catalysis[6,10–12] involving complexes of uranium. On the other hand, the public's negative associations attached to the word uranium are nurtured by sensational news from the press about nuclear weapons and energy politics as well as the radioactive waste management associated with these issues. As a consequence, uranium shares a reputation with other earth-abundant elements of the periodic table that are considerably more harmful, such as white phosphorus, beryllium, and mercury, all of which are slowly disappearing from chemical suppliers and research laboratories. All speculations aside, depleted uranium, in reality, is a weakly radioactive metal that can be handled easily and properly without any special precautions.

Fortunately, the lingering negative sentiments around uranium have not discouraged chemists from embarking on the mission to develop new chemistry of uranium and continue to transform a "waste product" into industrially relevant and environmentally safe compounds, thereby revealing fundamental new insights. The abundance of this element is also of great advantage with reports calculating the concentration of uranium to be 0.7 to 11 ppm in the soil[13] and approximately 2 to 4 ppm in the earth's crust,[13,14] 40 times more abundant than silver.

[a]*Department of Chemistry and Pharmacy, Inorganic Chemistry, University of Erlangen-Nürnberg, Egerlandstr. 1, D-91058 Erlangen, Germany. E-mail: karsten.meyer@chemie.uni-erlangen.de*
[b]*Department of Chemistry, University of California, San Diego, 9500 Gilman Drive, La Jolla, California 92093, USA*

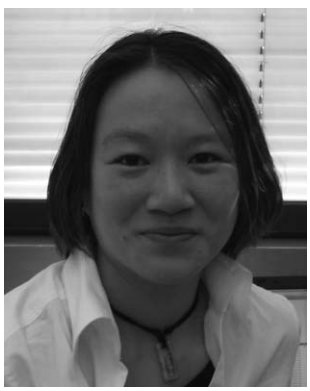

Oanh P. Lam

Oanh Phi Lam was born in 1982 in Saigon, Vietnam. In 2004, she received her BSc in Chemistry from the University of Washington, where she worked with Prof. Dr James Mayer. Her graduate education began at the University of California, San Diego (2005) with Karsten Meyer. Her research focuses on small molecule activation and functionalization at reactive uranium complexes supported by sterically encumbered macrocyclic ligands. In 2006, Oanh received her MSc in Chemistry from UCSD. Although still affiliated with UCSD, Oanh presently carries out her PhD research in the laboratories of Karsten Meyer at the University of Erlangen-Nuremberg in Erlangen, Germany.

Christian Anthon

Christian Anthon was born in 1973 in Frederikssund, Denmark. In 2001 he received his Cand Scient degree in Chemistry and Mathematics (University of Copenhagen). He continued his PhD studies in Copenhagen under Prof. Jesper Bendix (joint industrial project with Haldor Topsoe A/S). In July 2006 he received his doctorate from the University of Copenhagen, and in November 2006 the title of Industrial PhD. Since March 2007, Christian has been a postdoc in Karsten Meyer's group at the University of Erlangen-Nuremberg, where he investigates transition metal complexes of uranium with computational studies.

The increased interest in using uranium for coordination chemistry is due to certain unique chemical and physical properties that differentiate it from the transition metals, the lanthanides, and even the heavier actinides. In general, the 5f orbitals in actinides are less shielded by 6s and 6p electrons than the 4f orbitals in lanthanides by 5s and 5p electrons.[15] As a consequence, the 5f orbitals (Fig. 1) participate in covalent bonding much more readily than their 4f counterparts. However, this effect is more pronounced for lighter actinides than heavier ones, which possess more contracted f-orbitals and hence, behave more like lanthanides. Additionally, the large uranium ion can achieve higher coordination numbers compared to transition metals and, at the same time, the diffuse f-orbitals can support a wide range of oxidation states (+3 to +6) compared to the predominantly +3 oxidation state observed for lanthanides, and the high-valent oxidation states in actinyl species $[O{=}An{=}O]^{+/2+}$ with An = U, Pu, Np. Evidently, uranium holds a unique place in the periodic table that makes it an attractive candidate for coordination chemistry and as a catalytic agent.

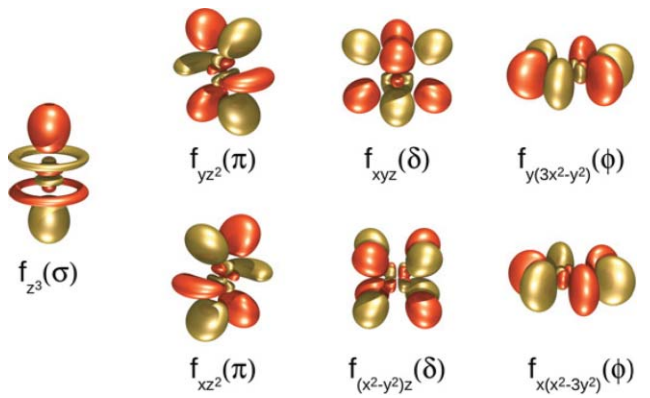

Fig. 1 The seven real 5f orbitals adapted to linear symmetry.

The 6d and 5f orbitals are similar in energy for the early actinide metals and mixed $7s^2 6d^1\ 5f^{n-1}$ ground state electron configurations are a common motif for the atomic actinides; however, progressing from left to right the main quantum number becomes more predominant, and the 5f orbitals correspondingly become more contracted, and significantly more stable than the 6d orbitals. The contraction of the 5f orbitals away from the valence region is strikingly noticeable in the atomic radii of the actinide metals, where a sudden volume increase is observed at plutonium, when progressing from left to right through the actinide metals.[16] This increase is caused by the loss of the 5f electrons from the metallic bonds.

While the 7s and 6d orbitals play a certain role in forming chemical bonds between the uranium ion in oxidation states III–VI, the valence region is dominated by the 5f orbitals, and the electron configurations are without exception $5f^n$ where n is 3 for U(III) and 0 for U(VI). The ligand field splitting of the 5f orbitals is found to be in the order of a few thousand cm^{-1}, which places the actinides in between the high values of the transition metals, where the ligand field is larger than the spin–orbit coupling, and the lanthanides, where the spin–orbit coupling is the dominating factor and the ligand field only plays a minor role. For the early actinide complexes, including those of uranium, the electronic ground state is determined by the interelectronic repulsion firstly, and it is therefore common to label the electronic ground state with the symbol of the matching f^n ion. For example, a uranium(IV) f^2 ion has a $^3H_4$ ground state, where the subscript 4 refers to the J quantum number, which for the ground states of the actinide metals with less than half filled f shells is found as the difference between $L(=5)$ and $S(=1)$. However, unlike the lanthanides, where the electronic states are dominated by the jj coupling scheme, and the transition metals where the electronic states are dominated by the ligand field, the similar magnitudes of the ligand field and the spin orbit coupling in the actinides give rise to magnetic data and electronic spectra that often defy explanation, let alone quantification.[15] In recent years, Kohn–Sham DFT with relativistic effects in form of the ZORA[17–20] method has added to the understanding of the electronic properties and the dynamics determining the structures of actinide complexes. Particularly interesting cases are the observation of a δ back-bond of in the inverted uranium-arene sandwich complex $[\{U(N(R)Ar)_2\}_2(\mu\text{-}C_7H_8)]$ ($R = CMe_3$, $Ar = 3,5\text{-}C_6H_3\text{-}Me_2$)[21] and the delocalization of the unpaired electron in the charged-separated ketyl uranium(IV) complex **5**.[22] In general, complexes with innocent ligands have structures that can be predicted with acceptable accuracy and some understanding of the metal–ligand bonds may be obtained.[22,23]

The bonding in Werner-type uranium complexes is well illustrated by the orbitals from a DFT computation of the *C*3 symmetric uranium(V) oxo complex $[((^{t\text{-}Bu}ArO)_3tacn)U(O)]$[23] (**30**, *vide infra*), where the bonding between the single oxo-ligand and uranium displays the typical polarity, and the corresponding low degree of participation of the uranium f orbitals (Fig. 2). We prefer to think of the uranium oxygen bond in **30** as formed between U^{5+} and an O^{2-} ion, which is not meant to imply that the bond is exclusively ionic, but rather as a convenient description. The unbound O^{2-} ligand has four lone-pairs, and we expect that three of these four lone-pairs interact with the uranium(V) center forming one σ bond and two π bonds. The last of the four oxide lone-pairs is non-bonding, and non-interacting, and points directly away from the uranium. The matching anti-bonding orbitals are the 7s, 6d and 5f orbitals of uranium. All of these orbitals are

Karsten Meyer

*Karsten Meyer was born in North Rhine-Westphalia, Germany (1968). In 1995 he received his diploma from the Ruhr-University in Bochum. He then began his graduate education with Prof. Karl Wieghardt at the Max-Planck-Institute for Bioinorganic Chemistry in Mülheim/Ruhr. His doctoral degree was awarded with distinction (*summa cum laude*) in January 1998. He then received a DFG postdoctoral fellowship with Prof. Christopher C. Cummins at MIT. In January 2001 he was appointed to the faculty at University of California, San Diego and was named an Alfred P. Sloan Fellow in summer 2004. In 2006, Karsten accepted the chair of inorganic chemistry and general chemistry at the University of Erlangen-Nuremberg.*

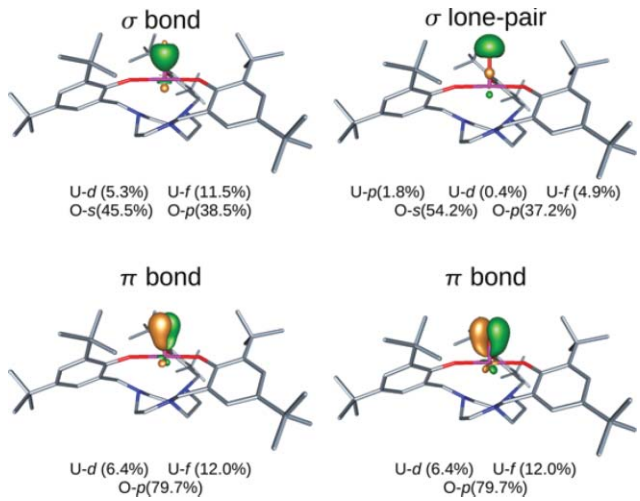

Fig. 2 Spin-restricted localized bonding orbitals in [(($^{t\text{-Bu}}$ArOH)$_3$tacn)-U(O)].

empty, except for the one unpaired f^1 electron of the uranium(V) ion. This electron is found in an fφ orbital, which is non-bonding with respect to the axially coordinated terminal oxide, situated in the plane of the three aryl-oxygens. Therefore, the one σ bond and two π bonds represent a complete picture of the uranium(V) oxygen bond, a formal triple bond. Both the σ and the π bonds are highly polarized, with oxygen participation of around 80%, while the uranium d and f orbitals of uranium account for the remaining 20%. The main uranium component in the bonds is, as expected, the 5f orbitals; however, the uranium 6d component is close to the half of that of the 5f orbitals, and the 6d orbital, must therefore be included to complete the bonding picture in this and most other uranium complexes. As stated above, this bonding motif is typical of uranium, where the bonds are mostly ionic, though not to the degree observed for the lanthanides, and not to a degree where the spectroscopically important 5f orbitals are unperturbed by the bonding.

While the organometallic chemistry of uranium is well developed,[24–27] reactivity of uranium complexes containing classical coordination ligands remains largely unexplored. This article will focus on the reactivity of uranium coordination complexes, with discussions involving manipulation of the ligand architecture to control uranium reactivity and the importance of steric pressure on promoting small molecule binding, activation, and functionalization. Emphasis will be placed on the reactivity of industrially relevant small molecules such as N_2, CO, and CO_2 with uranium complexes.

2. Syntheses of reactive U(III) coordination complexes

2.1 Ligand design

Macrocyclic chelating ligands have been used extensively to stabilize transition metal complexes.[28,29] A similar idea can be invoked in designing a classic Werner-type ligand that could support the large and extremely reactive uranium center, and simultaneously provide the controlled reactivity that is desired. Additionally, the ligand should have some features that can be readily modified in order to tailor the sterics of the resulting complex. Fig. 3 shows the macrocyclic hexadentate ligand platform with a triazacyclononane anchor functionalized by tris-aryloxide pendent arms, (^{R}ArOH)$_3$tacn (R = *t*-Bu, Ad), where the steric environment can be altered with different substituents such as *tert*-butyl or adamantyl groups at the aryl ortho positions. In addition, substituents in the aryl para positions such as the *tert*-butyl groups (Fig. 3, left) largely control the solubility. The (^{R}ArOH)$_3$tacn ligand system is aimed at stabilizing U(III) centers evident from three strong oxygen donors of the tris-aryloxide arms. The triazacyclononane anchor contains weak amine nitrogen donors and serves a dual purpose of protecting the underside of the uranium center from undesired reactions and further stabilization of the uranium center through weakly bound N-donors in a six-coordinate geometry.

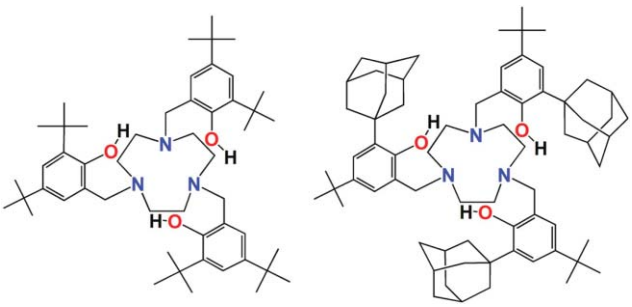

Fig. 3 Hexadentate tris-aryloxide ligands (^{R}ArOH)$_3$tacn with triazacyclononane as anchors.

2.2 Reactive U(III) precursor complexes

Upon coordination of the ligands, the six-coordinate [(($^{t\text{-Bu}}$ArO)$_3$tacn)U^{III}][30] (**1**) and [((^{Ad}ArO)$_3$tacn)U^{III}][31] (**2**) complexes (Fig. 4) feature the uranium centers coordinated in a distorted trigonal planar environment. This ligand arrangement around the uranium center creates a single reactive site at the free axial position, where small molecule binding and activation can occur. The molecular structures show that the U(III) center in the *tert*-butyl ligand system is placed 0.75 Å below the plane formed by the three oxygen atoms compared to 0.88 Å of that

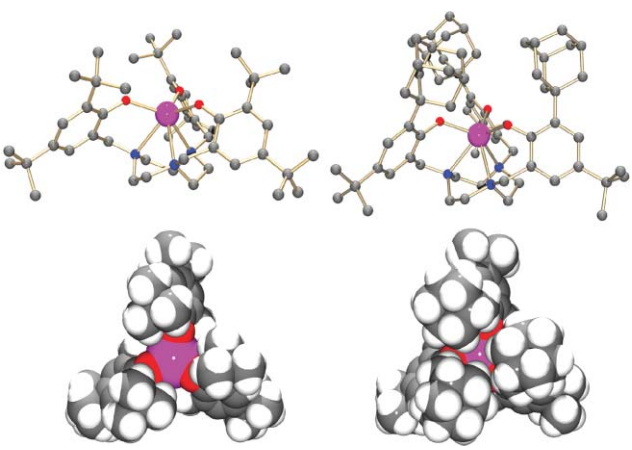

Fig. 4 Molecular structures of U(III) complexes **1** (left) and **2** (right) along with space-fill representations below.

observed for the U(III) center in the adamantyl ligand system. This phenomenon can be attributed to the van der Waals interaction within the adamantyl groups pushing the uranium center farther below the plane of the tris-aryloxide plane. When a seventh ligand (L) is coordinated, this uranium out-of-plane shift can be a good indicator of U–L_{ax} bonding strength and attractive electrostatic interactions. As U–L_{ax} orbital and electrostatic interactions increase, the uranium center gets pulled towards the tris-aryloxide plane. Average bond distances for **1**and **2** confirm strong U–O interactions with bond lengths of 2.238(4) Å and 2.224(9) Å and weak U–N interactions with longer bond lengths of 2.668(5) Å and 2.637(10) Å, respectively. The space filling models of **1** and **2** (Fig. 4) clearly illustrate the differences in size and shape of the reactive site as a direct consequence of the sterics of the ligands. The wide and shallow cavity of **1** results from a propeller-like arrangement of the *tert*-butyl groups, whereas the deeper and narrower cavity of **2** results from the perpendicular positioning with respect to the $(ArO)_3$ and van der Waals interactions of the sterically more encumbering adamantyl substituents. The differences in reactivity of these two U(III) complexes will be discussed in the following sections.

3. Charge-separated uranium complexes with radical anionic ligands: U^{IV}–$L^{\bullet -}$

Charge-separated complexes with radical anionic ligands are intriguing due to their unusual electronic and spectroscopic properties.[32–35] However, the difficulties regarding stabilization of such reactive compounds limit structural characterizations, and hence, many charge-separated complexes with radical anionic ligands have only been characterized *in situ via* spectroscopic methods.[36,37] Here, we demonstrate the ability of uranium complexes [$(({}^{R}ArO)_3tacn)U^{n+}$] to stabilize such compounds by combining the advantage of the sterically hindered $({}^{R}ArO)_3tacn^{3-}$ ligands with the propensity of U(III) centers to participate in one-electron reductions.

3.1 Activation of CO_2: a new coordination mode

Treatment of red-brown **1** with CO_2 gas (1 atm) promotes the splitting of CO_2 by a two-electron reduction process from two U(III) centers to form a pale-green, almost colourless dinuclear oxygen-bridged species [$\{(({}^{t\text{-Bu}}ArO)_3tacn)U\}_2(\mu\text{-O})$] (**3**) and simultaneous loss of CO (Scheme 1).[38] The dimerization process can be attributed to the lack of steric protection of the uranium provided by the three *tert*-butyl groups. In contrast, treating a red-brown toluene solution of **2** with the sterically bulkier adamantyl substituents with CO_2 gas (1 atm) results in immediate decolourization of the solution, indicating redox chemistry occurring upon reaction of U(III) with CO_2. Molecular and electronic structure studies confirm a new linear coordination mode of carbon dioxide, where the CO_2 fragment is bound to the uranium center in an η^1 fashion through the oxygen to form the charge-separated uranium complex with a radical anionic CO_2 fragment, [$(({}^{Ad}ArO)_3tacn)U(CO_2^{\bullet -})$] (**4**) (Fig. 5).[1] The η^1-OCO coordination mode had so far remained elusive; only other coordination modes of CO_2 have been reported such as Aresta's [$(Cy_3P)_2Ni(CO_2)$] (Cy = cyclohexyl)[39,40] and Herskovitz's [$(diars)_2M(CO_2)(Cl)$][diars = *o*-phenylenebis(dimethylarsine); M = Ir, Rh],[41] featuring the carbon-bound η^1-CO_2 and bidentate η^2-COO binding modes, respectively. IR spectroscopy of complex **4** shows a vibrational band corresponding to the υ_{OCO} stretch at 2188 cm^{-1} that shifts to 2128 cm^{-1} upon exposure to isotopically labelled $^{13}CO_2$ suggesting a reduced CO_2 when compared with the υ_{OCO} stretch of 2349 cm^{-1} in free CO_2. The reduction of CO_2 in **4** is also evident in the asymmetric C–O bond distances observed in the CO_2 unit, where one C–O bond is short at 1.122(4) Å and the other long at 1.277(4) Å. The observed C–O bond lengths within the CO_2 fragment can be described by

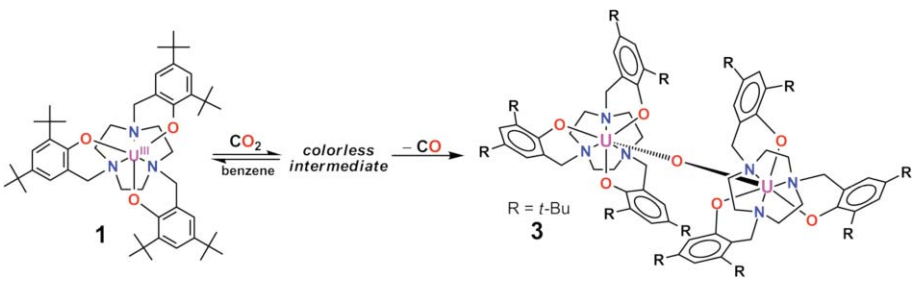

Scheme 1 Formation of dinuclear μ-O complex **3** *via* splitting of CO_2.

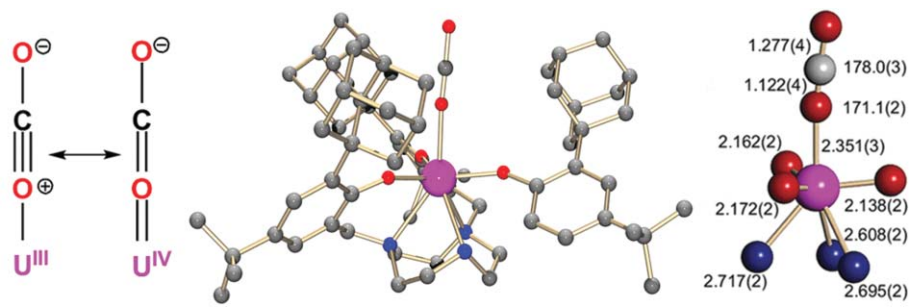

Fig. 5 Molecular structure of **4** and core bond distances and angles.

two resonance structures shown in Fig. 4. However, from the molecular structure alone, one cannot determine the uranium oxidation state in complex **4**. Assignment of uranium oxidation state can be quite complex for such species that have no precedence in the literature; nevertheless, it is crucial to understanding the extent that the CO_2 fragment is activated.

The distinguishing characteristics of complex **4** are best observed through variable-temperature SQUID magnetization data. At room temperature, it is difficult to differentiate U(IV) from U(III) species since both species exhibit similar effective magnetic moment (μ_{eff}) values of ~2.9μ_B. Differentiation is possible at 5 K, for instance, a U(IV) complex with a closed shell ligand, such as the azide ligand in U(IV)–N_3 (Fig. 5, blue), exhibits a low magnetic moment of ~0.6μ_B. due to non-magnetic ground state. By contrast a U(III) complex (Fig. 6, black) exhibits a much higher value of ~1.75μ_B due to a doublet ground state. Although the temperature dependence behaviour of complex **4** (Fig. 6, red) is similar to that of the U(IV)-N_3, the μ_{eff} value (~1.5μ_B. at 5 K) is indicative of a one-electron reduced CO_2 radical anionic ligand coordinated to a U(IV) ion, as in U^{IV}-$CO_2^{\bullet -}$.

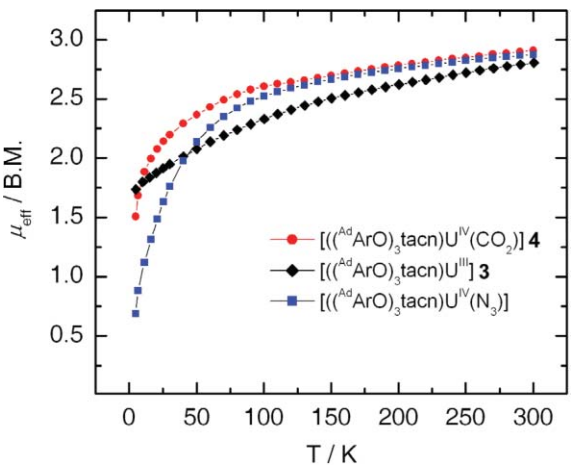

Fig. 6 Variable-temperature SQUID magnetization plot comparing U(IV) and U(III) species.

Formation of complex **4** is promoted by a highly reducing U(III) system supported by a stabilizing macrocyclic ligand. The ligand's steric influence *via* the adamantyl groups on the CO_2 fragment promotes the coordination of CO_2 in a linear fashion and illustrates the importance of ligand architecture on reactivity. By contrast, the U(III) system possessing the *tert*-butyl functionalized ligand does not succeed in stabilizing such $CO_2^{\bullet -}$ radical anionic species, leading to two-electron reduction and cleavage of CO_2.

3.2 Structural and spectroscopic investigations of a U-ketyl complex

Employing the sterically demanding macrocyclic ligand and trivalent uranium's propensity for one-electron reduction, a uranium benzophenone ketyl radical complex was stabilized and fully characterized. The treatment of **1** with 4,4′-di-*tert*-butylbenzophenone immediately yielded a purple product, which upon single crystal XRD analysis revealed complex **5** (Fig. 7, left).[22] The radical anionic nature of **5** can be demonstrated through further reaction with hydrogen donors, such as 1,4-cyclohexadiene to form the corresponding green methoxide product, complex **6** (Fig. 7, right). The molecular structure of **5** reveals the di-substituted benzophenone fragment coordinated through the oxygen and clearly shows an sp^2 ketyl carbon C70, confirming that a ketyl ligand fragment is stabilized. Complex **5** exhibits a relatively long U–O bond distance of 2.178(4) Å compared to those exhibited by U(IV)–O bonds (2.0–2.1 Å). The C–O bond distance of 1.334(6) Å in **5** suggests a bond that is intermediate between a single and double bond. Comparatively, in complex **6**, the U–O bond distance of 2.077(3) Å is consistent with a U(IV)–O single bond and the C–O bond distance of 1.406(5) Å agrees well with a C–O single bond. These metrical parameters can be explained by examining the four resonance structures that contribute to the overall molecular structure of **5** (Fig. 8). The first three resonance structures (**5a-5c**) describe the delocalization of the unpaired electron over the ketyl C2, ortho, and para carbons of the benzophenone unit. The last resonance structure depicts the unpaired electron localized on the uranium center, equivalent to a U(III) center with a coordinating benzophenone adduct. The contribution from the U(III) resonance structure in **5** effectively weakens the U–O bond while strengthening the C–O bond and hence, a difference in bond distances of complexes **5** and **6** is observed.

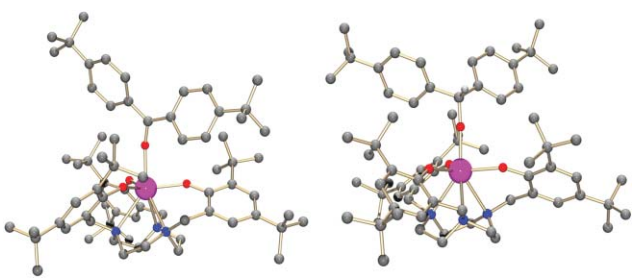

Fig. 7 Molecular structures of **5** (left) and **6** (right).

The unusual electronic properties of charge-separated complex **5** with a radical anionic benzophenone ligand can be observed

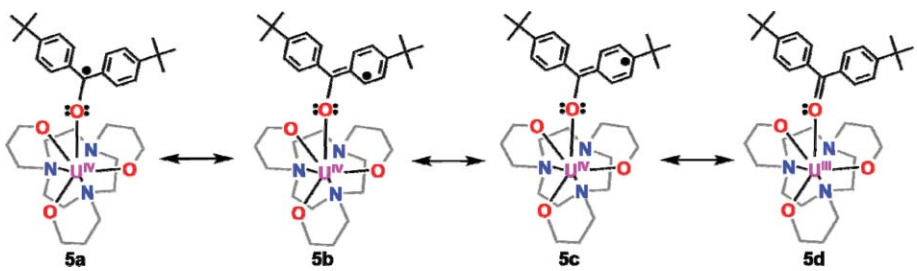

Fig. 8 Resonance structures of complex **5**.

simply by the intense deep purple colour that the complex exhibits. By contrast most U(IV) complexes of the [((R ArO)$_3$tacn)U] system are light green to colourless as exhibited by complex **6**. Electronic absorption data illustrates that the intense purple color is due to a π–π* transition of the highly conjugated benzophenone fragment in **5** (Fig. 9, top), which gets diminished upon hydrogen abstraction in **6** (Fig. 9, bottom). The weak absorptions along the vis-NIR region in **6** are assigned to metal centered Laporte forbidden f–f transitions of the uranium center.

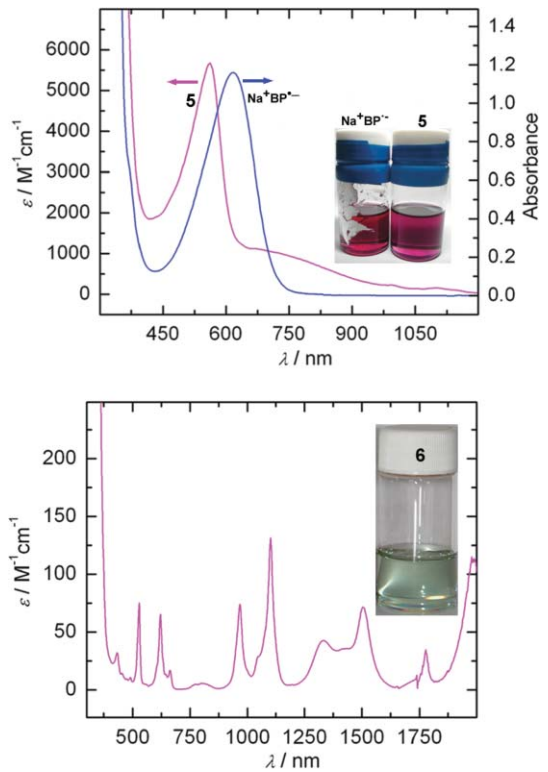

Fig. 9 Electronic absorption spectra of complexes **5** (top, magenta) with comparison to sodium benzophenone ketyl (top, blue) and complex **6** (bottom) in toluene.

As previously mentioned in the last section, variable temperature SQUID magnetization data is a reliable method for classifying compounds of the type U^{IV}–L$^{\bullet-}$. The low temperature magnetic moment (5 K, $\mu_{eff} = 1.61\mu_B$) of complex **5** (Fig. 10) is reminiscent of that of U–OCO$^{\bullet-}$ complex (**4**) (5 K, $\mu_{eff} = 1.50\mu_B$). The intermediate oxidation state of **5** is further confirmed through DFT studies. The Mulliken charge on the uranium of **5** is 1.46, between those found for [((t-Bu ArO)$_3$tacn)U^{III}] (**1**) (1.04) and U(IV) methoxide complex **6** (1.61). Similarly, the spin density on the uranium of 2.37 for complex **5** (Fig. 11) is also between those of **1** (3.11) and **6** (2.17) confirming the intermediate oxidation state between U(III) and U(IV) of **5**.

3.3 C–H activation of diphenyldiazomethane *via* a U^{IV}–N$_2$CPh$_2^{\bullet-}$ intermediate

The reactivity of the six-coordinate precursor complexes **1** and **2** with diphenyldiazomethane can be summed up with Scheme 2. Treating **1** with diphenyldiazomethane results in a charge-separated U(IV) complex bearing a radical anionic Ph$_2$CN$_2^{\bullet-}$ unit.

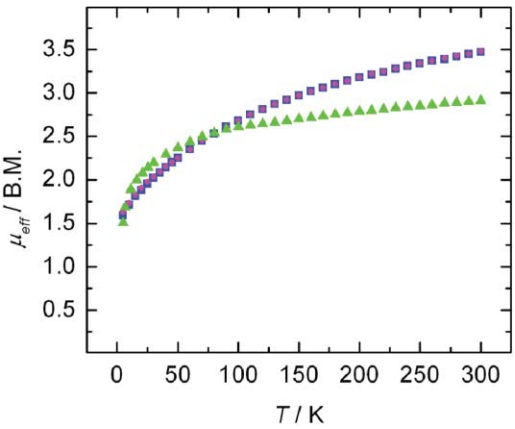

Fig. 10 Temperature-dependent SQUID magnetization data for **5** (magenta, blue) plotted along with **4** (green) for comparison. Spin density plot of **5** is shown at bottom.

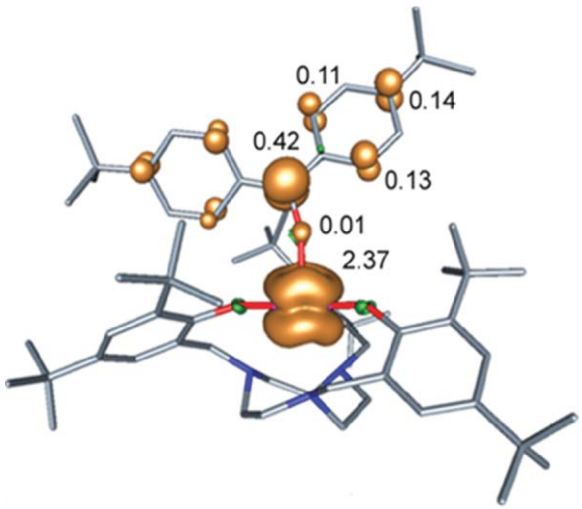

Fig. 11 Spin density plot of complex **5**.

XRD analysis on the orange single crystal revealed the diphenyldiazomethane ligand coordinated in an η^2 fashion (**7**) (Fig. 12, left).[42]

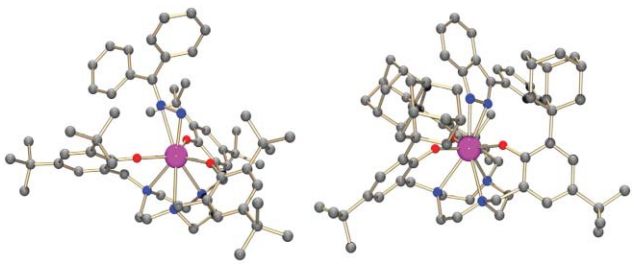

Fig. 12 Molecular structures of complexes **7** (left) and **9** (right).

The reaction of more sterically demanding **2** with diphenyldiazomethane proceeds through two intermediates (**8** and **8a**) resulting in the final formation of a green uranium indazole complex. The molecular structure of the heterocyclic indazole complex (**9**) shows the 3-phenyl indazole unit coordinated in an η^2 fashion with the planar indazole fragment wedged between two adamantyl groups of the ligand (Fig. 12, right).[42] Intermediate **8** can be

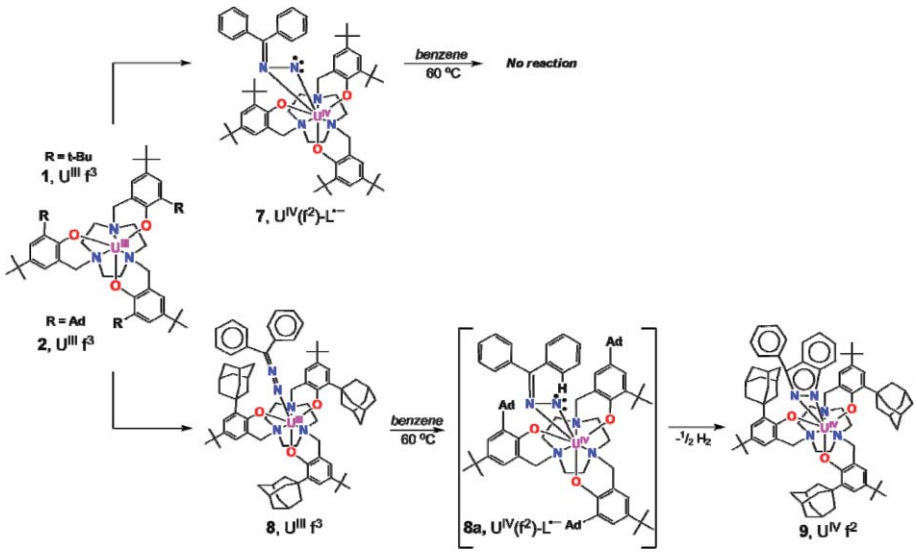

Scheme 2 Synthetic pathway for complexes **7** and **9**.

isolated; however, structural characterization was not possible due to its highly reactive nature. Although the transformation occurs at room temperature, heating **8** at 60 °C in benzene results in complete transformation to indazole complex **9** within one hour. Formation of **9** proceeds *via* intermediate **8a** (not isolable), which bears an α-N (N4) with significant radical character. This reactive α-N (N4) promotes the C–H activation, subsequent N-insertion, and hydrogen elimination ($\frac{1}{2}$ equiv.) to generate the heterocyclic indazole complex **9**.

It should be emphasized that heating **7** at 60 °C in benzene gives no further reaction even when the reaction is allowed to proceed for days. A closer examination of the molecular structure of **9** in space-fill representation helps explain the difference in reactivity between the two ligand systems (Fig. 13). The rare transformation from **8** to **9** is attributed to the steric pressure exerted on the diphenyldiazomethane fragment by the adamantane groups (and possibly a weak π–π interaction), thereby placing a phenyl ring in plane with the N–N–U plane and allowing the electron-rich imido-type α-N (N4) closer to the ortho phenyl C–H bond for insertion. For this reason, the less sterically pressured **7** does not undergo nitrogen insertion when heated because the phenyl groups are allowed to freely rotate making N-insertion into the C–H bond entropically unfavourable.

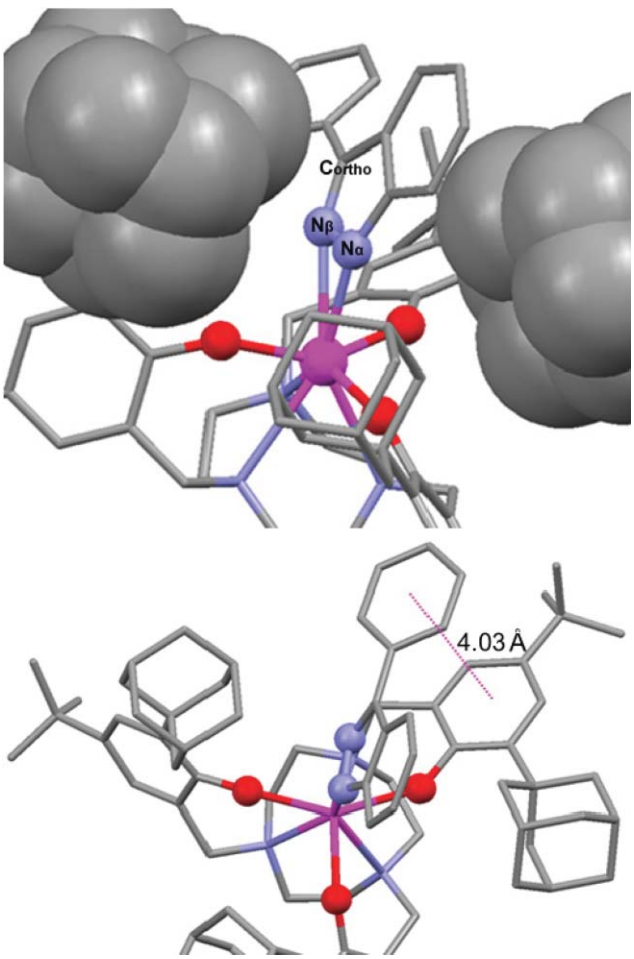

Fig. 13 Space-fill representation of **9** (top) and aryl π–π interaction (bottom).

4. Small molecule coordination, activation and functionalization by uranium

Transformation of simple abundant chemical feedstock, such as dinitrogen, carbon monoxide, and carbon dioxide to more industrially relevant compounds is arguably one of the present time's most important goals.[43–45] The most challenging aspect relates to the stability of the multiple bonds these compounds possess. Often times, success depends on achieving the balance of having a highly reducing metal complex that can also stabilize the activated unit and prevent it from decomposition or undesirable transformations. Besides its one- and multi-electron reducing capabilities, uranium possesses various binding modes, which makes this early f-element a great candidate for activation of such compounds.

4.1 Dinitrogen coordination and activation

The dinitrogen triple bond is arguably one of the most difficult bond to activate, as evidenced by the harsh temperature and pressure conditions required for the Haber–Bosch process.[46] Remarkably, Haber reported that uranium metal or even $(UN)_x$ materials were found to be the best catalysts for the conversion of N_2 to NH_3 to date (1909).[46] There are several examples of uranium dinitrogen complexes demonstrating that this metal has the ability to bind and possibly activate the extremely inert N_2 bond. The first uranium dinitrogen complex was synthesized from a low-valent U(III) complex supported by a tripodal tris-amide ligand system, [U(NN′$_3$)] where NN′$_3$ = N(CH$_2$CH$_2$NSiBu^{t}Me$_2$)$_3$ (**10**). Treating trivalent **10** with 1 atm of N_2 results in dinitrogen coordinated in a side-on bridging fashion between two uranium centers, **11** (Scheme 3).[47] When freeze-thaw degassing procedures are performed on **11**, conversion back to **10** is observed, demonstrating that this N_2 binding process is reversible. The N–N bond in **11** of 1.109(7) Å is nearly identical to that in N_2 gas (1.10975 Å), indicating little or no activation of the dinitrogen unit.

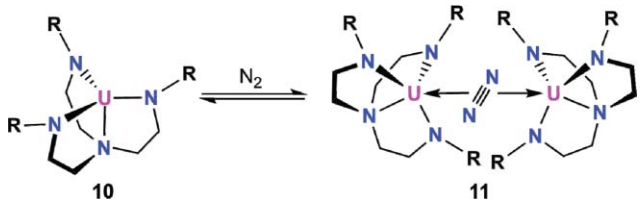

Scheme 3 Synthetic route to complex **11**.

It has been suggested that the preference for side-on binding of N_2 is facilitated by better N–N bond activation *via* electron density donation from uranium π orbitals into the N_2 π* orbital.[48–50] Dinitrogen binding of [U(NN′$_3$)] is most likely promoted by the tripodal triamidoammine with the sterically bulky silyl substituents creating the appropriate geometry and pre-organizing the complex for side-on binding of N_2.

Reduction of dinitrogen was successful when trivalent uranium pentalene complex [U(Cp*)(C$_8$H$_4${Si^{i}Pr$_3$-1,4}$_2$)] (**12**) was used. Upon treating **12** with 1 atm of N_2, side-on coordination occurs to give an η^2-N_2 bridged dimeric uranium complex [{U(Cp*)(C$_8$H$_4$(Si^{i}Pr$_3$-1,4)$_2$)}$_2$(μ:η^2,η^2-N$_2$)] (**13**) (Scheme 4).[51] Reversible dinitrogen binding was also observed in this case. The N–N bond in **13** of 1.232(10) Å is consistent with an N–N double bond and is the result of a two-electron reduction from two U(III) centers giving rise to two U(IV) centers with a bridging N_2^{2-} ligand.

End-on binding mode of dinitrogen has also been documented for uranium, most notably in the formation of heterodinuclear [(U)Mo(μ-N$_2$)] complex. When trivalent Mo complex

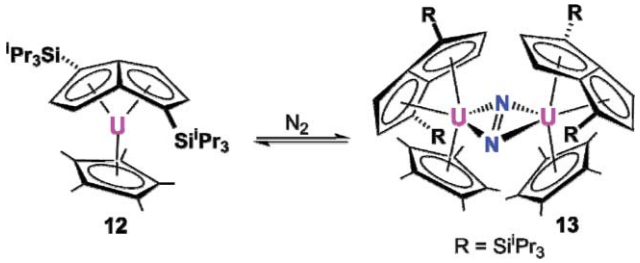

Scheme 4 Reduction of dinitrogen by a trivalent uranium pentalene complex.

[Mo(N(*t*-Bu)(Ph))$_3$] (**15**) is exposed to 1 atm of N_2, presumably, a molybdenum dinitrogen complex [(N$_2$)Mo(N[*t*-Bu]-Ph)$_3$] is generated and gets trapped by trivalent uranium precursor [U(THF)(N(*t*-Bu)(Ar))$_3$] (Ar = 3,5-dimethylphenyl) (**14**) to form an end-on bound dinitrogen heterodinuclear complex [(Ar[*t*-Bu]N)$_3$U(μ:η^2,η^2-N$_2$)Mo(N[*t*-Bu]Ph)$_3$] (**16**) (Scheme 5).[52] Structural data reveals an N–N bond of 1.232(11) Å confirming a reduced N_2 with an N–N bond order of 2. The short Mo–N bond distance of 1.773(8) Å suggests a Mo–N double bond and a relatively short U–N bond distance of 2.220(9) Å indicates some degree of U–N multiple bonding.

The reversibility of dinitrogen binding in **11** and even **13**, where the N_2 fragment is significantly reduced, illustrates well the hurdle that needs to be surpassed in order to further activate dinitrogen and functionalize it. In the case of **11**, although the ligand is "pre-organized" towards side-on N_2 binding, the dinitrogen ligand is simply not reduced enough to be stabilized. A much more reduce N_2^{2-} is achieved in **13**, however, it has been suggested that the reversibility of dinitrogen binding is the result of steric relief due to the bulky substituents on the pentalene ligand.[51] Although the preferred formation of a terminal nitride complex [N≡Mo(N(Ar)(*t*-Bu))$_3$] has been reported,[53] **16** is thermally stable, perhaps due to the difficulty of generating a U(VI) in absence of an appropriate stabilizing ligand system. Hence, the challenge of functionalizing dinitrogen lies in finding a suitable, yet flexible, ligating environment along with a highly reducing metal center. In these regards, uranium has great potential. Due to its large size and f-orbital involvements in bonding, the uranium ion can support a variety of coordination numbers, geometries, and oxidation states. Although synthesized in an N_2 atmosphere, complexes **1** and **2** do not form isolable N_2 complexes, however solvent variation and high-pressure studies are under way.

4.2 Carbon monoxide binding and activation

Carbon monoxide is an important industrial feedstock for syntheses of hydrocarbons and oxygenates through the Fischer–Tropsch

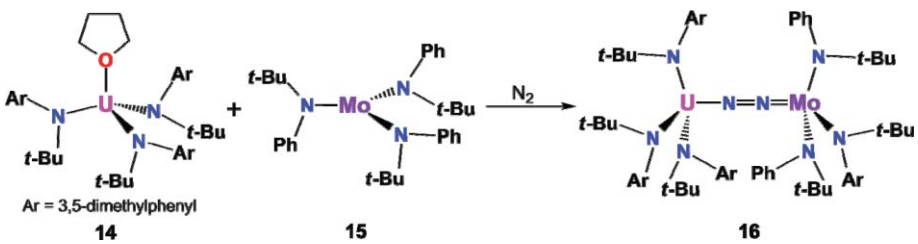

Scheme 5 Synthesis of end-on bound dinitrogen complex of uranium and molybdenum.

process that was discovered in the 1930's.[54] Since then, there has been a lot of interest in activating carbon monoxide using highly reducing metal centers.[55] Electron-rich uranium complexes are promising candidates for activation of carbon monoxide due to their reducing power and their abilities to stabilize charge-separated species with radical anionic ligands, as presented in the previous section. The following section will present carbon monoxide activation by low-valent and high-valent uranium complexes, further show casing an impressive versatility of (organometallic) uranium coordination chemistry.

4.2.1 CO activation by low-valent U(III). Synthesis of the first uranium carbon monoxide complex [(η^5-$Me_3SiC_5H_4)_3U(CO)$], involved treating [(η^5-$Me_3SiC_5H_4)_3U$] with CO gas.[56] The CO absorption band of the complex is exhibited at 1976 cm^{-1} and shifts to 1935 cm^{-1} when isotope labelled ^{13}CO is used. However, when vacuum is applied to the carbon monoxide complex, decomposition to the starting trivalent uranium complex occurs, indicating that CO binding is reversible. The reversible binding of CO does not occur with the ($^{R}ArOH_3$)tacn ligand system. Treating **1** with CO results in an end-on CO bridged mixed-valent U(IV)/U(III) dinuclear complex [{(($^{t\text{-}Bu}ArO)_3$tacn)U}$_2$(μ-CO)] (**17**) (Scheme 6).[38] XRD studies confirm the formation of the complex but, because the CO fragment lies on a crystallographic inversion center, no reliable C–O bond distance was obtained. Formation of dinuclear **17** is believed to occur by nucleophilic attack of a charge-separated [(($^{t\text{-}Bu}ArO)_3$tacn)U-$CO^{\bullet-}$] on a coordinatively unsaturated **1**. As mentioned previously, the uranium out-of-plane shift within the ($^{R}ArO)_3$tacn ligand system is an indication of U–L_{ax} interactions, and thus, can often hint at the oxidation state of the uranium. For instance, the uranium center in the U(IV)–N_3 lies 0.32 Å below the tris-aryloxide plane compared to 0.44 Å for a U(III)-$NCCH_3$. Comparatively, the uranium center in complex **17** lies 0.38 Å below the tris-aryloxide plane, supporting the average oxidation state of the U centers of +3.5 and suggesting a mixed-valent U(III)/U(IV) complex. Furthermore, the mixed-valent U(III)/U(IV) complex [{(($^{t\text{-}Bu}ArO)_3$tacn)U}$_2$(μ-N_3)], synthesized from treating [(($^{t\text{-}Bu}ArO)_3$tacn)$U^{IV}(N_3)$] with [(($^{t\text{-}Bu}ArO)_3$tacn)U^{III}] (**1**), featured the uranium center at 0.37 Å below the tris-aryloxide plane, nearly coinciding with the corresponding value in **17**.[38]

Further functionalization of CO has been reported, notably with the homologation of carbon monoxide using uranium organometallic complexes. Cyclotrimerization of CO occurs to give a diuranium deltate complex, [(U($COT^{\dagger}$)(Cp^{*}))$_2$(μ:η^2,η^2-C_3O_3)] († = 1,4-bis(tri-isopropylsilyl)) (**19**), when [U($COT^{\dagger}$)$_2$-(Cp^{*})(THF)] (**18**) is treated with 1 bar of CO at room temperature (Scheme 7, top).[3] The C_3O_3 dianion is evidently formed from a two-electron reduction of three equiv of CO, one-electron reduction, each at two U(III) centers. The C–O bonds of the deltate dianion range from 1.26 to 1.30 Å and are between a C–O single bond (1.43 Å) and a C–O double bond (1.21 Å). The C–C bond between the η^2 bound oxygen atoms is longer (1.436 Å) than the other two C–C bonds (1.377 Å and 1.381 Å). DFT calculations suggest a C–C agostic interaction with the uranium center that is most likely responsible for the distortion within the three-membered ring. Slight changes in the ligand architecture of the U(III) complex alters the reactivity significantly, and consequently, results in the formation of a diuranium squarate complex, [(U($COT^{\dagger}$)(Cp^{Me4H}))$_2$(μ:η^2,η^2-C_4O_4)] (**21**), upon exposing **20** to CO (Scheme 7, bottom).[57] The C_4O_4 unit in **21** is planar as expected and the bond distances are comparable to the η^2-bound fragment of **19**. However, the U–C bonds are much longer than in **19** indicating the lack of agostic C–C interactions. Supported by DFT studies, the formation of **19** and **21** is believed to occur through addition of excess CO to a "zig-zag" uranium ynediolate intermediate complex U–O–C–C–O–U.[58]

The difference in reactivity of **18** and **20** emphasizes the important role that ligand architecture and steric pressure play. Generally, it has been noted before that the sterically bulkier [U(η-$Cp^{*})_3$] system is more reactive than the [U(η-$Cp^{Me4H})_3$] system.[59,60] By contrast, the less sterically bulky [(($^{t\text{-}Bu}ArOH)_3$tacn)U] (**1**) is generally more reactive than [(($^{Ad}ArOH)_3$tacn)U] (**2**) as shown with the splitting of CO_2 in section 3.1. However, it is with the [(($^{Ad}ArOH)_3$tacn)U] system that further chemistry was observed with regards to functionalization of diphenyldiazomethane. Hence, it is important to bear in mind that often times, small changes in ligand environment can have significant effects on reactivity and that one cannot consistently predict the direction of reactivity when the sterics are altered.[61–63]

4.2.2 CO activation with high-valent U(V). Activation of carbon monoxide by high-valent U(V) complexes is less commonly documented than with low-valent U(III) complexes. Carbon monoxide inserts into the U–C double bond of U(V) complex [$(Cp)_3U(=CHPMePh_2)$] forming a β-ketoylide [$(Cp)_3U(\eta^2$-$COCHPMePh_2)$] complex.[64] Activation of CO can also be achieved with adamantyl derivatized [(($^{Ad}ArO)_3$tacn)U($NSiMe_3$)] (**22**) (Fig. 14, left), a U(V) imido complex formed from treating **2** with trimethylsilyl azide.[65,66] Molecular structure of **22** displays a seven-coordinate complex with a bent trimethylsilyl imide unit with a U–N–Si angle of 162.55(12)°. By contrast, the analogous *tert*-butyl derivatized [(($^{t\text{-}Bu}ArO)_3$tacn)U($NSiMe_3$)] (**24**) (Fig. 14, right) exhibits a more linear imide unit with a U–N–Si angle of 178.5(3)°. Accordingly, the U–N bond distance in **22** is the longest

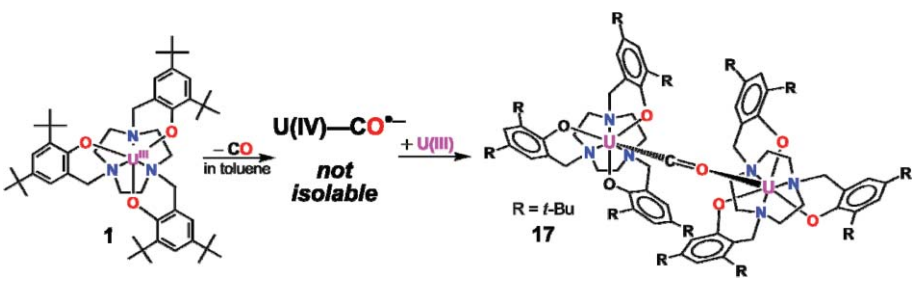

Scheme 6 Formation of a mixed-valent U(IV)/U(III) μ-CO complex.

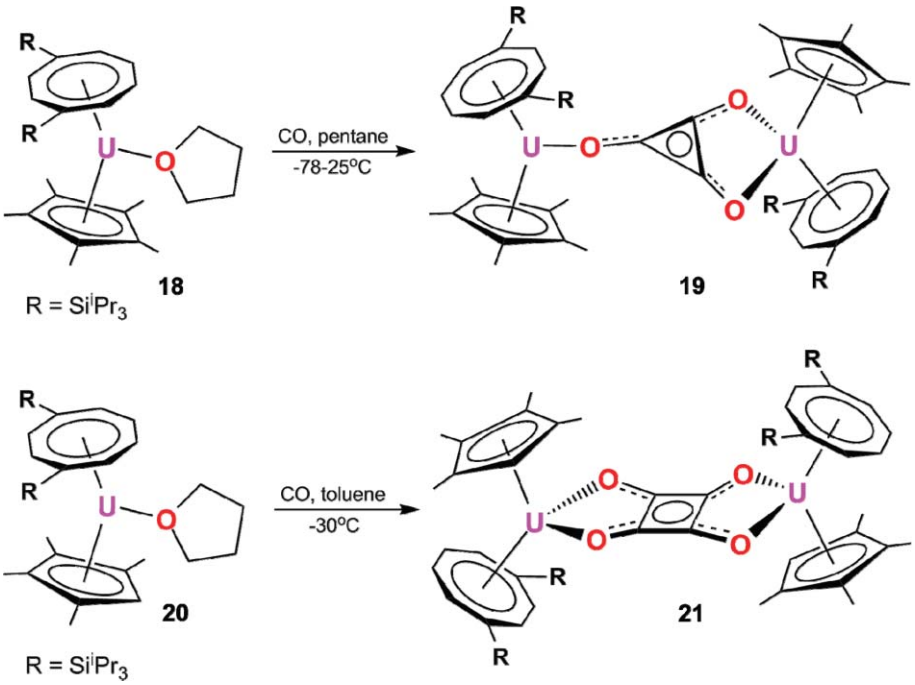

Scheme 7 Synthesis of diuranium deltate (**19**) and squarate (**21**) complexes.

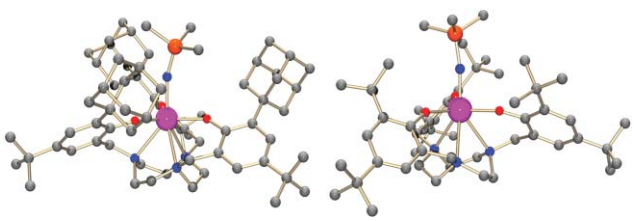

Fig. 14 Molecular structures of **22** (left) and **24** (right).

ever reported for a U(V) imide complex at 2.1219(18), Å while the U–N bond length in **24** is characteristically short at 1.985(5) Å. The unusual features of **22** are most likely due to the steric pressure exerted on the imido fragment by the bulky adamantyl groups preventing the Me_3SiN^{2-} unit from optimal binding. Consequently, complex **22** reacts with π-acids, such as methyl isocyanide and carbon monoxide to form the corresponding U(IV) carbodiimide and isocyanate complex [((^{Ad}ArO)$_3$tacn)U(NR)] (where R = CNR, CO); **23** for R = CO) with concomitant elimination of $Me_3Si\cdots SiMe_3$ (Scheme 8), whereas complex **24** is unreactive towards CO. It should be noted that **22** also reacts with CH_3NC to form a U(IV) carbodiimide complex, with release of Me_6Si_2.[66] The reactivity of **22** compared to unreactive **24** can most definitely be attributed to the bent trimethylsilyl imide unit caused by steric pressure of the adamantyl groups. This steric pressure is directly visible in the crystal structures, where **22** has a longer U–N bond and a larger deviation from linearity with regards to the U–N–Si moiety. DFT calculations suggest a high degree of ionic character within the U^{5+}-NR^{2-} fragment, which further explains the reactivity **22** as compared to group 6 transition metal complexes that possess more covalent (less polarized) and less reactive metal–ligand multiple bonds.

4.3 Carbon dioxide binding and activation

Much progress has been achieved concerning the activation of carbon dioxide with transition metals.[67–69] However, little is known about the reactivity of carbon dioxide with regards to the f-block elements. There have been some examples of carbon dioxide functionalization using La, Ce, Pr, Nd, and Sm systems.[70,71] Employing low-valent complexes of early f-block elements, such as uranium, is also promising due to their oxophilicity and propensity to participate in one- or multi-electron redox processes. Although there are few examples of CO_2 binding and activation by uranium, the examples discussed in the following section demonstrates that uranium, when coupled with suitable ligating environments, can provide the optimum platform for CO_2 activation and unusual transformations.

4.3.1 CO_2 activation by low-valent U(III) and mid-valent U(IV). Activation of carbon dioxide with a low-valent U(III) complex has been discussed in section 3.1 with formation of the end-on bound charge-separated uranium CO_2 complex [((^{Ad}ArO)$_3$tacn)U($CO_2^{\bullet-}$)] (**4**) from treatment of the U(III) precursor **2** with 1 atm of CO_2.[1] Hence, this section will further showcase uranium's flexibility by highlighting the activation of CO_2 with mid-valent U(IV) complexes.

It has been reported that carbon dioxide can insert into the U–S bond of a U(IV) dithiolate complex [(η^5-C_5Me_5)$_2$U(S^{t}Bu)$_2$] to form the thiocarboxylate product [(η^5-C_5Me_5)$_2$U(O_2CS^tBu)$_2$], which represents the first isolated structure of a complex formed from the insertion of CO_2 into a metal–sulfur bond.[72] In this case, carbon dioxide insertion was reversible, demonstrated by extrusion of CO_2 from the inserted product upon thermolysis. Other remarkable instances document the insertion of carbon dioxide into a U–N amide bond of U(IV) mesityl amide complexes [(($^{t\text{-}Bu}$ArO)$_3$tacn)U(NHMes)] (**25**) and [((^{Ad}ArO)$_3$tacn)U(NHMes)]

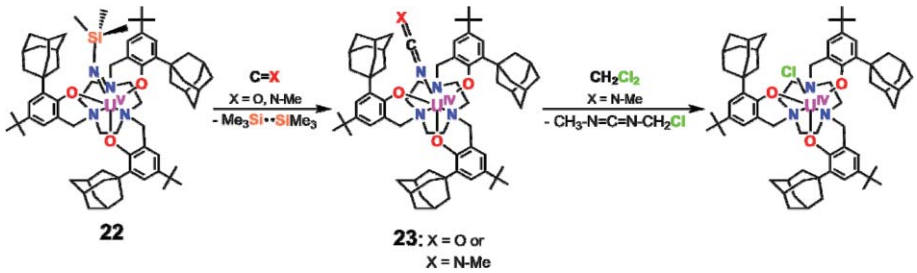

Scheme 8 Formation of **23** from multiple-bond metathesis of CO.

(**27**) (Scheme 9). Syntheses of **25** and **27** are achieved *via* H_2 elimination through simple treatment of **1** and **2** with 2,4,6-trimethylaniline at 100 °C, respectively.[23] The tetravalent U–N bond distance obtained from the molecular structure of **25** of 2.305(6) Å is long compared to U–N bonds of other uranium amide complexes such as $[(\eta^5\text{-}C_5Me_5)_2U(Cl)(NH(p\text{-}C_6H_5Cl))]$[73] and $[(\eta^5\text{-}C_5Me_5)_2U(NH(2,6\text{-}Me_2C_6H_3))]$[74] of 2.237(3) Å and 2.267(6) Å, respectively. The unusually long U–N bond is likely a contributing factor to the reactivity of this complex. Treatment of **25** with 1 atm of CO_2 yields the CO_2 inserted monodentate carbamato complex $[(({}^{t\text{-}Bu}ArO)_3tacn)U(\eta^1\text{-}OC(O)N\text{-}(H)Mes)]$ (**26**). Similarly, complex **27** can also undergo CO_2 insertion to form $[(({}^{Ad}ArO)_3tacn)U(\kappa^2\text{-}O_2CN(H)Mes)]$ (**28**) where the carbamato ligand is bound in a κ^2 fashion. The insertion of CO_2 into a U(IV)–amide bond is rare but has been reported previously with $[(\eta^5\text{-}C_5H_5)_2U(NEt_2)_2]$ to form the corresponding carbamato species, $[(\eta^5\text{-}C_5H_5)_2U(O_2NEt_2)_2]$.[75]

The difference in coordination modes can clearly be observed in the molecular structures of **26** and **28** (Fig. 15). The different preferences in binding of the carbamato ligands can be attributed to the steric differences in the macrocyclic ligand framework. The monodentate carbamato complex **26** features a short U–O bond of 2.227(3) Å, which is significantly shorter than the two U–O bonds of bidentate carbamato **28** of 2.434(4) Å and 2.527(4) Å. The *tert*-butyl groups in **26** create a much more open cavity, and hence, allow the carbamato ligand better access to the uranium center to form *one* strong U–O bond. The much more bulky adamantyl groups in **28**, however, prevent the carbamato ligand from optimum binding to the uranium center, and consequently, as a compensation for this, *two* weaker U–O bonds are formed.

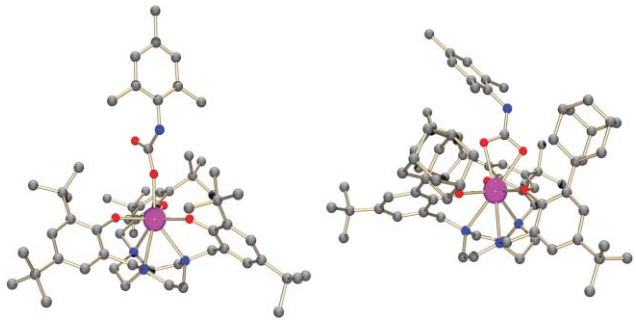

Fig. 15 Molecular structures of **26** (left) and **28** (right).

4.3.2 CO_2 activation by high-valent U(V) complexes: formation of $U^V{\equiv}O$. The reactivity of the U(V) imide complex **22**, reported in section 4.2.2, demonstrates the great potential of the $[(({}^{R}ArO)_3tacn)U^V(NR)]$ platform to undergo unusual chemical transformations. Accordingly, the reactivity of $[(({}^{R}ArO)_3tacnU)(NMes)]$ were also explored with regards to carbon dioxide activation. Pentavalent uranium imide complexes $[(({}^{t\text{-}Bu}ArO)_3tacnU)(NMes)]$ (**29**) and $[(({}^{Ad}ArO)_3tacnU)(NMes)]$ (**31**) can be synthesized from treating **1** and **2** with 1 equiv. of mesityl azide (Scheme 10).[23] The molecular structure of **29**

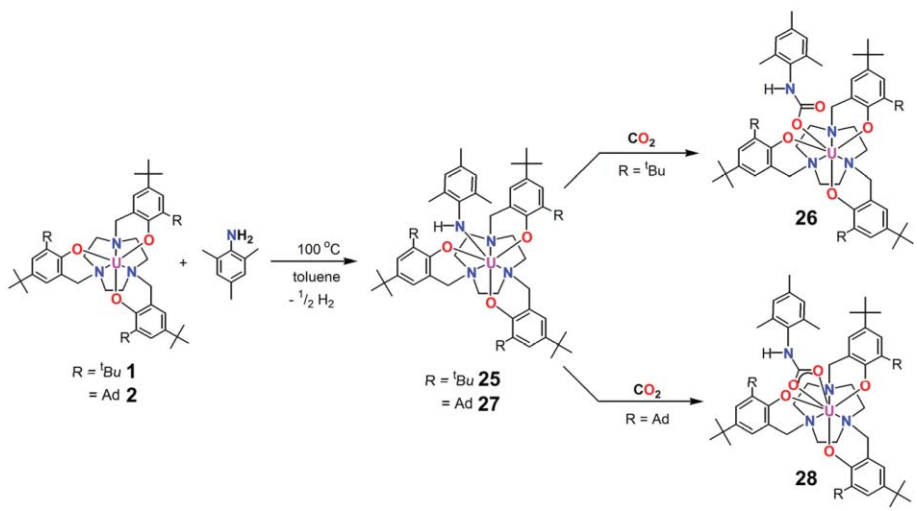

Scheme 9 Insertion of CO_2 into U–N amide bonds in formation of **26** and **28**.

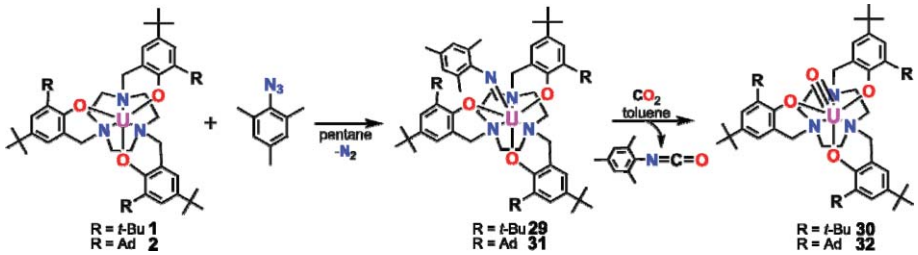

Scheme 10 Formation of U(v) terminal oxo species **30** and **32**.

reveals a seven-coordinate complex with a bent mesityl imide fragment featuring a U–N–C angle of 154.7(8)°, contrasting the nearly linear U–N–Si angle in [((t-BuArO)$_3$tacn)U(NSiMe$_3$)] (**24**) of 178.5(3)°. Correspondingly, the U–N bond in **29** of 2.047(8) Å is slightly longer than that in **24** of 1.985(5) Å. The bent mesityl imide and longer U–N bond of **29** are reminiscent of the bent trimethylsilyl imide unit of **22**, which has been shown as the likely source of reactivity towards π-acids. Although no structural data were obtained for **31**, presumably, the mesityl imide unit there is also bent. The evidence for this is demonstrated in the reactivity of **29** and **31** with carbon dioxide to form the corresponding U(v) terminal oxo species [((t-BuArO)$_3$tacn)U(≡O)] (**30**) and [((AdArO)$_3$tacn)U(≡O)] (**32**), respectively (Scheme 10). Formation of terminal oxo species **30** and **32** occurs through insertion of carbon dioxide into the U=N bond of **29** and **31**, driven by elimination of the thermodynamically stable U≡O triple bond and the mesityl isocyanate fragment. The transformations are postulated to occur through a [2 + 2] cycloaddition and multiple-bond metathesis; a process well documented for transition metals.[76–84] The molecular structures of **30** and **32** (Fig. 16) indeed reveal terminal oxo species, where the respective U–O bond distances are very short at 1.848(8) Å, which are comparable to only one other crystallographically characterized monomeric U(v) terminal oxo species, [(Cp*)$_2$(OMes)U(O)] (1.859(6) Å).[85] Although the uranium terminal oxo group is common for the uranyl class [O=U=O]$^{2+}$, formation of monomeric U(v) terminal monooxo compounds are rare, and most importantly, are not accessible by the commonly accepted route of treating a U(iii) complex with an oxygen-atom transfer reagent; the latter will lead to μ-oxo (in case of **1**) and hydroxo U(iv) species (in case of **2**), respectively.

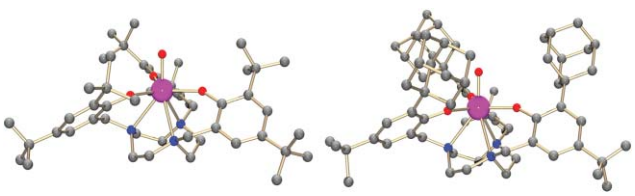

Fig. 16 Molecular structures of **30** (left) and **32** (right).

The uranium carbimato intermediate complex formed during the course of [2 + 2] cycloaddition of CO_2 was not isolable due to the rapid release of the mesityl isocyanate fragment. This occurrence can be ascribed to the steric bulk of the mesityl group facilitating the loss of the isocyanate. To test this hypothesis, the less sterically hindered phenyl azide was utilized for synthesis of the U(v) phenyl imide complex [((t-BuArO)$_3$tacn)U(NPh)] (**33**), with an aim at trapping the uranium carbimato intermediate. Treating **33** with 1 atm of CO_2 yields a uranium diphenyl ureate derivative [((t-BuArO)$_3$tacn)U(κ^2-*N*,*N*-(NPh)$_2$CO)] (**34**). The molecular structure of **34** (Fig. 17) displays an eight-coordinate complex with the diphenyl ureate ligand coordinated through the two nitrogen atoms. The U–N bond distances are measured at 2.329(4) and 2.310(4) Å, indicative of single bonds. Although the uranium carbimate intermediate was not obtained, formation of **34** confirms that the route to the uranium terminal oxo complexes **30** and **32** passes through a uranium carbimato complex. However, due to the highly reactive nature of such carbimato complexes, a second [2 + 2] cycloaddition event occurs with another equivalent of uranium(v) phenyl imide species to form an N,O-coordinated diphenyl ureate, which subsequently isomerizes to the final *N*,*N*-coordinated diphenyl ureate complex **34**. An alternative route may involve the initial formation of the U(v) terminal oxo species **30** and PhNCO, which could react with the remaining complex **33** to form **34**.[23]

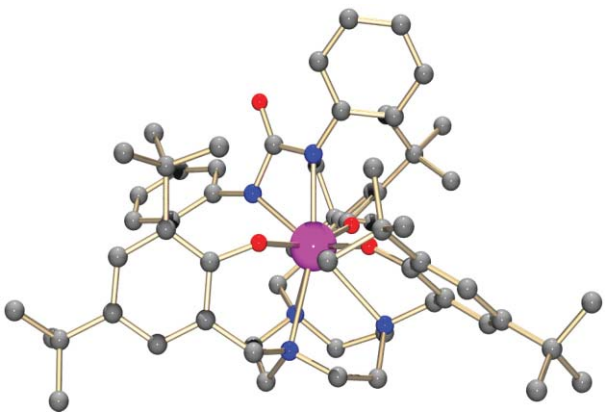

Fig. 17 Molecular structure of **34**.

In addition to being rare, the U(v) terminal oxo complexes **30** and **32** possess very unusual spectroscopic and electronic properties. For instance, the electronic absorption data of **30** feature four broad low intensity bands at λ_{max} = 1770 nm (ν = 5650 cm^{-1}, ε = 70 cm^{-1}M^{-1}), 1480 nm (ν = 6769 cm^{-1}, ε = 90 cm^{-1}M^{-1}), 1205 nm (ν = 8300 cm^{-1}, ε = 75 cm^{-1}M^{-1}), and 850 nm (ν = 11765 cm^{-1}, ε = 50 cm^{-1}M^{-1}) (Fig. 18, top-right). Absorptions in the region ranging from ~800 nm to ~2000 nm with extinction coefficient ranging from 25 cm^{-1}M^{-1} are due to f–f transitions often observed for lanthanide and actinide complexes.[15] These four distinct bands are unprecedented for the complexes of the [((RArO)$_3$tacn)U] system. The four bands presumably arise from the ^{2}F manifold, where the 5f electron is

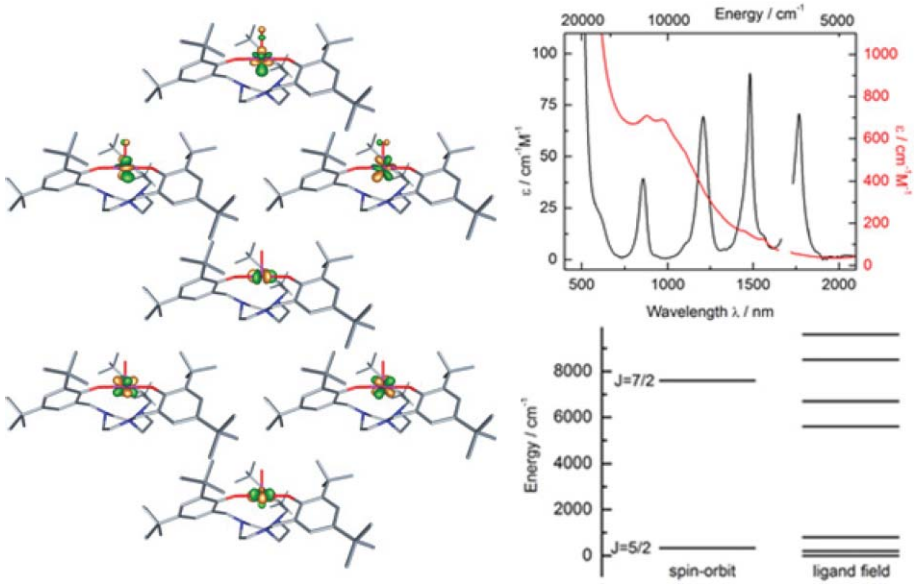

Fig. 18 Electronic absorption spectrum of **30** (top, black) overlaid with **29** (top, red) for comparison and energy level schematic for a $5f^1$ system assuming the spin–orbit interaction is greater than the ligand field interaction. Left: The seven α f orbitals in **30**, the SOMO and 6 LUMOs.

split by 5f spin–orbit interaction into two J multiplets, $J = 5/2$, $7/2$. The two J multiplets will be further split by the crystal field into $(2J + 1)/2$ doubly degenerate levels (Kramer doublets). With the approximation that complexes **30** and **32** are of C_{3v} symmetry, the $J = 5/2$ level spits into two $\mu = 1/2$ doublets and one $\mu = 3/2$ doublets.[86] Assuming that the spin–orbit effects are much larger than the ligand field effects, a schematic can be produced for the $5f^1$ system (Fig. 18, bottom-right). From this energy level diagram, it can be expected that the optical transitions will occur between 5500–10 000 cm^{-1}, which were observed for **30** and **32**.

The HOMO and LUMO orbitals of a spin unrestricted scalar ZORA DFT ground state computation of oxo complex **30** are easily examined in terms of ligand field theory. The complex is a trigonal planar with an additional oxo ligand placed directly above the uranium center. We expect that the three orbitals that are σ and π antibonding with respect to the oxo ligand are the three LUMOs with highest energy. The remaining four of seven f orbitals are unperturbed by the oxo ligand. The two δ orbitals are degenerate. They interact with the π orbitals of the aryloxy oxygen perpendicular to the plane. The two ϕ orbitals are non-degenerate; one interacts in a σ fashion and the other in a π fashion with the aryloxides. From a simple ligand field argument, we would expect σ interactions to be larger than π interactions, and thus, we expect one of the three π interaction orbitals to form the ground state. However, the σ interacting orbital is stabilized by s–f and d–f mixing to a degree that makes it the HOMO, carrying the one unpaired electron of the f^1 complex.

Unexpectedly, complexes **30** and **32** were found to be EPR active, a contrast to isoelectronic U(V) imide complexes that have been reported, which are all EPR silent. An X-band EPR analysis of toluene/acetonitrile glass of **32** at 8 K revealed an axial system with g-values at $g_z = 2.15$ and $g_{xy} = 1.14$ (Fig. 19). As mentioned, in C_{3v} symmetry, the $J = 5/2$ splits into three magnetic doublets, two EPR active $\mu = \pm 1/2$ and one EPR inactive $\mu = \pm 3/2$, where μ is the crystal ground-state number. Hence, it is postulated that

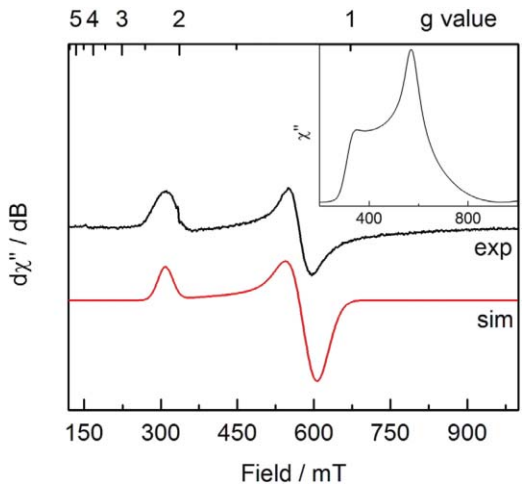

Fig. 19 X-Band EPR spectrum of **32** recorded in toluene–acetonitrile glass at 5 K ($\nu = 9.40187$ GHz, $P = 0.10$ mW, modulation = 3.0 mT at 100 kHz). Inset shows the numerical integration of the experimental derivative spectrum.

complexes **30** and **32** must have crystal ground-states of $\mu = 1/2$.[87] By contrast, the uranium(V) complexes $[(\eta^5\text{-}MeC_5H_4)_3U(NR)]$ and $[\{\eta^5\text{-}MeC_5H_4)_3U\}_2(\mu\text{-}N_2C_6H_4)]$ have $\mu = 3/2$ crystal field ground state and therefore are EPR silent.[87,88] Accordingly, U(V) imide complexes of the [((RArO)$_3$tacn)U] system, such as **22**, **24**, **29**, and **31**, are also EPR inactive.

The reactivity of [((t-BuArO)$_3$tacnU(NMes))] (**29**), which features a bent imide unit, towards π-acids compared to the analogous inert [((t-BuArO)$_3$tacnU(NSiMe$_3$))] (**24**), where the imide fragment is nearly linear, demonstrates that the steric environments in both the ligand and the substrate are important. Through careful manipulation of both, one can discover new reaction pathways that will lead to formation of unusual compounds.

5. Conclusions and perspectives

Employing uranium as a metal in coordination chemistry is a very promising prospect. The involvement of the 5f orbitals in covalent bonding sets it aside from the lanthanide and heavier actinide metals. The large uranium ion is advantageous for supporting a number of ligands and coordination modes, which makes it more versatile than most transition metals. Furthermore, the wide range of oxidation states that uranium possesses (U^{III} to U^{VI}) is useful for one- and multi-electron processes necessary for small molecule activation and functionalization. However, the challenge in harvesting uranium's reducing capabilities lies in stabilizing and controlling the reactivity of the highly reactive trivalent U(III) ion. As covered in this article, the ligands that show promise, thus far, incorporate sterically bulky substituents that can protect the uranium center from unwanted side reactions, while simultaneously provide a single controlled reactive site where chemistry can occur. Having the possibility to sterically modulate the ligand is also beneficial, demonstrated by the formation of end-on bound CO_2 [$(^{Ad}ArO)_3tacn)U(CO_2^{\bullet-})$] (**4**) upon replacing the *tert*-butyl groups in **1** with adamantyl groups in **2** and the formation of diuranium squarate complex **21** by exchanging a Cp* ligand for less sterically hindered Cp^{Me4H} ligand. The influence sterics put on substrates can be very significant, as shown with the promotion of C–H activation and N-insertion of diphenyldiazomethane by the adamantyl groups to form the uranium indazole complex **9**. This phenomenon is also exhibited in the U(V) imide complex [$(^{Ad}ArO)_3tacn)U(NSiMe_3)$] (**22**), where the steric pressure put on by the adamantyl groups causes the imide unit to bend and the U–N bond to weaken. As a result, complex **22** is reactive towards π-acids, while complex **24** is inert. Similarly complex **29** and **31**, both featuring bent mesityl imide fragments further react with CO_2, forming rare examples of U(V) terminal oxo complexes **30** and **32** otherwise not accessible.

The versatility of uranium has been demonstrated by its reactivity towards small molecules in a variety of oxidation states with trivalent, tetravalent, and pentavalent uranium. We have witnessed that, when the appropriate ligating environment for uranium is engineered, inert molecules, such as N_2, CO, and CO_2, can be activated and functionalized under mild conditions. Furthermore, the exemplary capacity of uranium to stabilize charge-separated complexes implies its potential for facilitating catalytic processes by stabilizing highly reactive intermediates evolving out of catalytic transformations. These findings are very encouraging for the future of uranium coordination and catalytic chemistry. Hence, the continuous search for suitable ligand systems is a worthy endeavour, and perhaps soon, uranium will find its niche back in university chemistry education, chemistry laboratories, and ultimately, in industrial applications, provided that the anti-nuclear sentiments of the public can be dissolved.

Acknowledgements

The authors wish to thank Dr Ingrid Castro-Rodriguez, Dr Hidetaka Nakai, and Dr Suzanne Bart for their contributions to the uranium coordination chemistry presented in this article. Research was supported by grants from the U. S. Department of Energy (DOE grant DE-FG02-O4ER 15537), DFG, and SFB 583. This research was also supported in part by NSF Grant CHE05–18707 (J. M. O.).

References

1 I. Castro-Rodriguez, H. Nakai, L. N. Zakharov, A. L. Rheingold and K. Meyer, *Science*, 2004, **305**, 1757–1760.
2 W. J. Evans, S. A. Kozimor and J. W. Ziller, *Science*, 2005, **309**, 1835–1838.
3 O. T. Summerscales, F. G. N. Cloke, P. B. Hitchcock, J. C. Green and N. Hazari, *Science*, 2006, **311**, 829–831.
4 T. W. Hayton, J. M. Boncella, B. L. Scott, P. D. Palmer, E. R. Batista and P. J. Hay, *Science*, 2005, **310**, 1941–1943.
5 P. L. Arnold, D. Patel, C. Wilson and J. B. Love, *Nature*, 2008, **451**, 315–317.
6 A. R. Fox, S. C. Bart, K. Meyer and C. C. Cummins, *Nature*, 2008, **455**, 341–349.
7 P. M. Almond, M. L. McKee and T. E. Albrecht-Schmitt, *Angew. Chem., Int. Ed.*, 2002, **41**, 3426–3429.
8 J. T. Lyon, H.-S. Hu, L. Andrews and J. Li, *Proc. Natl. Acad. Sci. U. S. A.*, 2007, **104**, 18919–18924.
9 N. Kaltsoyannis and P. Scott, *Chem. Commun.*, 1998, 1665–1666.
10 E. Barnea and M. S. Eisen, *Coord. Chem. Rev.*, 2006, **250**, 855–899.
11 J. W. Bruno, M. R. Duttera, C. M. Fendrick, G. M. Smith and T. J. Marks, *Inorg. Chim. Acta*, 1984, **94**, 271–277.
12 C. J. Weiss, S. D. Wobser and T. J. Marks, *J. Am. Chem. Soc.*, 2009, **131**, 2062–2063.
13 J. Emsley, *Nature's Building Blocks: An A–Z Guide to the Elements*, Oxford University Press, USA, 2001.
14 F. Weigel, *McGraw-Hill Encyclopedia of Science and Technology*, 5th edn, McGraw-Hill Book Co., Inc., New York, 1987, vol. 19, pp. 75–81.
15 T. J. Marks, *Prog. Inorg. Chem.*, Vol. 25, John Wiley & Sons, New York, 1979.
16 K. T. Moore and G. von der Laan, *Rev. Mod. Phys.*, 2009, **81**, 235–64.
17 E. Van Lenthe, E. J. Baerends and J. G. Snijders, *J. Chem. Phys.*, 1993, **99**, 4597–4610.
18 E. Van Lenthe, E. J. Baerends and J. G. Snijders, *J. Chem. Phys.*, 1994, **101**, 9783–9792.
19 E. Van Lenthe, A. E. Ehlers and E. J. Baerends, *J. Chem. Phys.*, 1999, **110**, 8943–8953.
20 G. te Velde, F. M. Bickelhaupt, S. J. A. van Gisbergen, C. Fonseca Guerra, E. J. Baerends, J. G. Snijders and T. Ziegler, *J. Comput. Chem.*, 2001, **22**, 931–967.
21 P. L. Diaconescu, P. L. Arnold, T. A. Baker, D. J. Mindiola and C. C. Cummins, *J. Am. Chem. Soc.*, 2000, **122**, 6108–6109.
22 O. P. Lam, C. Anthon, F. W. Heinemann, J. M. O'Connor and K. Meyer, *J. Am. Chem. Soc.*, 2008, **130**, 6567–6576.
23 S. C. Bart, C. Anthon, F. W. Heinemann, E. Bill, N. M. Edelstein and K. Meyer, *J. Am. Chem. Soc.*, 2008, **130**, 12536–12546.
24 M. Ephritikhine, *Dalton Trans.*, 2006, 2501–2516.
25 D. Seyferth, *Organometallics*, 2004, **23**, 3562–3583.
26 M. Sharma and M. S. Eisen, *Structure and Bonding*, Springer-Verlag, Berlin Heidelberg, 2008, vol. 127.
27 O. T. Summerscales and F. G. N. Cloke, *Structure and Bonding*, Springer-Verlag, Berlin Heidelberg, 2008, vol. 127.
28 L. F. Lindoy, *Chem. Soc. Rev.*, 1975, **4**, 421–441.
29 J. D. Chartres, L. F. Lindoy and G. V. Meehan, *Coord. Chem. Rev.*, 2001, **216–217**, 249–286.
30 I. Castro-Rodriguez, K. Olsen, P. Gantzel and K. Meyer, *Chem. Commun.*, 2002, 2764–2765.
31 H. Nakai, X. Hu, L. N. Zakharov, A. L. Rheingold and K. Meyer, *Inorg. Chem.*, 2004, **43**, 855–857.
32 W. J. Evans and D. K. Drummond, *J. Am. Chem. Soc.*, 1989, **111**, 3329–3335.
33 N. M. Edelstein, P. G. Allen, J. J. Bucher, D. K. Shuh and C. D. Sofield, *J. Am. Chem. Soc.*, 1996, **118**, 13115–13116.
34 M. Schultz, J. M. Boncella, D. J. Berg, T. D. Tilley and R. A. Andersen, *Organometallics*, 2002, **21**, 460–472.
35 K. Wieghardt, *Progress in Inorganic Chemistry*, John Wiley & Sons, Inc., New York, 2002, vol. 50.
36 Z. Hou, A. Fujita, Y. Zhang, T. Miyano, H. Yamazaki and Y. Wakatsuki, *J. Am. Chem. Soc.*, 1998, **120**, 754–766.
37 K. J. Covert, P. T. Wolczanski, S. A. Hill and P. J. Krusic, *Inorg. Chem.*, 1992, **31**, 66–78.

38 I. Castro-Rodriguez and K. Meyer, *J. Am. Chem. Soc.*, 2005, **127**, 11242–11243.
39 M. Aresta, C. F. Nobile, V. G. Albano, E. Forni and M. Manassero, *J. Chem. Soc., Chem. Commun.*, 1975, 636–637.
40 M. Aresta and C. F. Nobile, *J. Chem. Soc., Dalton Trans.*, 1977, 708–711.
41 T. Herskovitz, *J. Am. Chem. Soc.*, 1977, **99**, 2391–2392.
42 O. P. Lam, P. L. Feng, F. W. Heinemann, J. M. O'Connor and K. Meyer, *J. Am. Chem. Soc.*, 2008, **130**, 2806–2816.
43 G. A. Olah, A. Goeppert, and S. G. K. Prakash, *Beyond Oil and Gas: The Methanol Economy*, Wiley-VCH, Weinheim, 2006.
44 W. B. Tolman, *Activation of Small Molecules*, Wiley-VCH, Weinheim, 2006.
45 M. Aresta and A. Dibenedetto, *Dalton Trans.*, 2007, 2975.
46 F. Haber, Ammonia, *Ger. Pat.*, DE 229 126, 1909.
47 P. Roussel and P. Scott, *J. Am. Chem. Soc.*, 1998, **120**, 1070–1071.
48 B. A. MacKay and M. D. Fryzuk, *Chem. Rev.*, 2004, **104**, 385–402.
49 J. A. Pool, W. H. Bernskoetter and P. J. Chirik, *J. Am. Chem. Soc.*, 2004, **126**, 14326–14327.
50 P. J. Chirik, *Dalton Trans.*, 2007, 16–25.
51 F. G. N. Cloke and P. B. Hitchcock, *J. Am. Chem. Soc.*, 2002, **124**, 9352–9353.
52 A. L. Odom, P. L. Arnold and C. C. Cummins, *J. Am. Chem. Soc.*, 1998, **120**, 5836–5837.
53 C. E. Laplaza, M. J. A. Johnson, J. C. Peters, A. L. Odom, E. Kim, C. C. Cummins, G. N. George and I. J. Pickering, *J. Am. Chem. Soc.*, 1996, **118**, 8623–8638.
54 C. K. Rofer-DePoorter, *Chem. Rev.*, 1981, **, 81**, 447–474.
55 K. G. Moloy and T. J. Marks, *J. Am. Chem. Soc.*, 1984, **, 106**, 7051–7064.
56 J. G. Brennan, R. A. Andersen and J. L. Robbins, *J. Am. Chem. Soc.*, 1986, **108**, 335–336.
57 O. T. Summerscales, F. G. N. Cloke, P. B. Hitchcock, J. C. Green and N. Hazari, *J. Am. Chem. Soc.*, 2006, **128**, 9602–9603.
58 A. S. Frey, F. G. N. Cloke, P. B. Hitchcock, I. J. Day, J. C. Green and G. Aitken, *J. Am. Chem. Soc.*, 2008, **130**, 13816–13817.
59 W. J. Evans, G. W. Nyce and J. W. Ziller, *Angew. Chem., Int. Ed.*, 2000, **39**, 240–242.
60 W. J. Evans, S. A. Kozimor and J. W. Ziller, *J. Am. Chem. Soc.*, 2003, **125**, 14264–14265.
61 J. A. Pool, E. Lobkovsky and P. J. Chirik, *Nature*, 2004, **427**, 527–530.
62 Y.-C. Tsai, F. H. Stephens, K. Meyer, A. Mendiratta, M. D. Gheorghiu and C. C. Cummins, *Organometallics*, 2003, **22**, 2902–2913.
63 D. V. Yandulov and R. R. Schrock, *Science*, 2003, **301**, 76–78.
64 R. E. Cramer, R. B. Maynard, J. C. Paw and J. W. Gilje, *Organometallics*, 1982, **1**, 869–71.
65 I. Castro-Rodriguez, H. Nakai and K. Meyer, *Angew. Chem., Int. Ed.*, 2006, **45**, 2389–2392.
66 I. Castro-Rodriguez and K. Meyer, *Chem. Commun.*, 2006, 1353–1368.
67 X. Yin and J. R. Moss, *Coord. Chem. Rev.*, 1999, **181**, 27–59.
68 J. Louie, J. E. Gibby, M. V. Farnworth and T. N. Tekavec, *J. Am. Chem. Soc.*, 2002, **124**, 15188–15189.
69 M. Takimoto and M. Mori, *J. Am. Chem. Soc.*, 2002, **124**, 10008–10009.
70 W. J. Evans, D. B. Rego, J. W. Ziller, A. G. DiPasquale and A. L. Rheingold, *Organometallics*, 2007, **26**, 4737–4745.
71 W. J. Evans, C. A. Seibel and J. W. Ziller, *Inorg. Chem.*, 1998, **37**, 770–776.
72 F. Calderazzo, G. Dell'Amico, R. Netti and M. Pasquali, *Inorg. Chem.*, 1978, **17**, 471–473.
73 R. G. Peters, B. L. Scott and C. J. Burns, *Acta Crystallogr., Sect. C: Cryst. Struct. Commun.*, 1999, **55**, 1482–1483.
74 T. Straub, W. Frank, G. J. Reiss and M. S. Eisen, *J. Chem. Soc., Dalton Trans.*, 1996, 2541–2546.
75 A. L. Arduini, J. D. Jamerson and J. Takats, *Inorg. Chem.*, 1981, **20**, 2474–2479.
76 P. Jernakoff, G. L. Geoffroy, A. L. Rheingold and S. J. Geib, *J. Chem. Soc., Chem. Commun.*, 1987, 1610–1611.
77 R. S. Pilato, C. E. Housmekerides, P. Jernakoff, D. Rubin, G. L. Geoffroy and A. L. Rheingold, *Organometallics*, 1990, **9**, 2333–2341.
78 U. Kusthardt, W. A. Hermann, M. L. Ziegler, T. Zahn and B. Nuber, *J. Organomet. Chem.*, 1986, **311**, 163–175.
79 O. Blacque, H. Brunner, M. M. Kubicki, J.-C. Leblanc, W. Meier, C. Moise, Y. Mugnier, A. Sadorge, J. Wachter and M. Zabel, *J. Organomet. Chem.*, 2001, **634**, 47–54.
80 F. R. Lemke, D. L. DeLaet, J. Gao and C. P. Kubiak, *J. Am. Chem. Soc.*, 1988, **110**, 6904–6906.
81 D. L. DeLaet, R. del Rosario, P. E. Fanwick and C. P. Kubiak, *J. Am. Chem. Soc.*, 1987, **109**, 754–758.
82 B. D. Ward, G. Orde, E. Clot, A. R. Cowley, L. H. Gade and P. Mountford, *Organometallics*, 2005, **24**, 2368–2385.
83 D. J. Darensbourg, B. J. Frost and D. L. Larkins, *Inorg. Chem.*, 2001, **40**, 1993–1999.
84 M. H. Chisholm and M. W. Extine, *J. Am. Chem. Soc.*, 1977, **99**, 782–792.
85 D. S. J. Arney and C. J. Burns, *J. Am. Chem. Soc.*, 1993, **115**, 9840–9841.
86 G. F. Koster, J. O. Dimmock, R. G. Wheeler and H. Statz, *Properties of the Thirty-Two Point Groups*, MIT Press, Cambridge, MA, 1963.
87 R. K. Rosen, R. A. Andersen and N. M. Edelstein, *J. Am. Chem. Soc.*, 1990, **112**, 4588–4590.
88 J. G. Brennan and R. A. Andersen, *J. Am. Chem. Soc.*, 1985, **107**, 514–516.